Journal of Himalayan Earth Sciences Volume 56, No. 1, 2023 pp. 11-32

Microfacies and Depositional Settings of the Eocene Nisai Formation, Pishin Belt, Pakistan

Abdullah Abdullah[1], Mohibullah Mohibullah[2*], Aimal Khan Kasi[1], Shams ul Alam[1,3], Ejaz ul Haq[3]

[1]Centre of Excellence in Mineralogy, University of Baluchistan, Quetta

[2]Department of Geology, University of Baluchistan, Quetta

[3]Oil and Gas Development Company Limited, Pakistan

**Corresponding Author Email. mohibullah.kakar@um.uob.edu.pk*

Submitted date: 15/01/2023 Accepted date: 24/03/2023 Published online: 31/03/2023

Abstract

The Eocene Nisai Formation of the Pishin Belt at its type section represents thick carbonate-siliciclastics, deposited in an intermittent sub-basin between Eurasian and Indian plates on the north-western margin of Pakistan. These carbonates contain rich assemblages of Larger Benthic Foraminifera (LBF) (Discocyclina, Operculina, Alveolina, Assilina, milliolids, Nummulites etc.), smaller benthic, planktonic foraminifera and other fossil assemblages such as molluscs, brachiopods, bryozoans, algae etc. Microfacies of the Nisai Formation have been studied using biota along with the lithological characters and sedimentary textures. Eight carbonate microfacies have been recognized representing deposition in an inner ramp to outer ramp settings. The association of abundant Nummulties, Assilina, lenticular Discocyclina and algae along with quartz grains at places represent a mid-ramp setting developed as result of episodic relative sea level fall, enhanced continental weathering and tectonic uplift. Flattened Discocyclina, Operculina, Nummulities, smaller benthic foraminifera, planktonic foraminifer accumulation indicates an outer ramp setting and milliolids contribute shallow marine inner ramp environment.

Keywords: Nisai Formation, Microfacies, Larger Benthic Foraminifera, Planktonic Foraminifera, Depositional Environment, Pishin Belt

1. Introduction

The early Paleogene was a time of active tectonics and extreme global warming which caused perturbation in marine environments (Zachos et al., 2001). The marine shallow water environments were mainly occupied by larger benthic foraminifera (LBF), algae and corals (Hottinger, 1997, 1998; Afzal et al., 2011a, 2011b). These extreme warming conditions and increased sea surface temperatures of the Eocene caused decline of the coral reefs by expelling the temperature sensitive endosymbionts zooxanthellae from coral tissues (Payros et al., 2010). The decline in coral reef rimmed platforms provided an opportunity to LBF to flourish in the stressed environments as LBF modified their life strategy by adapting adult dimorphism and increasing their test size, thus paving way for the development of widespread carbonate ramp system (Hottinger, 1998; Hallock, 2001; Scheibner and Speijer, 2008). LBF being the major component of the Eocene carbonate platforms and one of the major carbonate producers have shown greater diversification owing to their sensitivity to light, temperature, sea water chemistry, water depth and substrate which made them one of the most useful tool to reconstruct the palaeodepositional settings along with other biogenic (molluscs, algae, corals etc) and abiogenic components (Hottinger, 1998; Pomar and Hallock, 2008).

The Paleogene strata in Pakistan is represented by excellent outcrops in the Indus Basin and the Pishin Belt. The Palaeocene-Eocene succession of the Indus Basin of Pakistan has received attention for modern biostratigraphic and palaeoecological studies for the last two decades (Warraich et al., 2000; Afzal et al., 2009, 2011a, 2011b; Hanif et al., 2014; Babar et al., 2018; Rehman et al., 2018; Ishaq et al., 2019; Uddin et al., 2019; Kamran et al., 2021) but the palaeontological data from the Eocene of the Pishin Belt, Pakistan is still scant and is poorly understood despite the excellent outcrops of the Eocene Nisai Formation. The Nisai Formation was formed after the emplacement of Ophiolites during Eocene-

Oligocene and is exposed throughout the Pishin Belt, particularly on the northern and southern sides of the Zhob Valley. The formation represent thick marine succession attaining a thickness of more than 900 m in some areas such as the type locality and consists of thin to thick bedded, nodular, reefoidal limestone, mudstones, sandstone and conglomerate. The limestone at many places is rich in fossil such as corals, foraminifera, echinoderms, bryozoans, molluscs, algae and ichnofossils. But despite the presence of various facies and rich faunal assemblages, the formation is still loosely defined in terms of age and palaeodepositional settings. However, some recent studies have given some details of the biostratigraphy and depositional setting of the Nisai Formation. Recently, Bukhari et al., (2016) have documented diverse LBF from the type section of the Nisai Formation and dated the formation as Middle to Late Eocene based on the presence of Asterigerina rotula, Assilina sublaminosa, As. leymeriei, As. subspinosa, Sphaerogypsina globula, Austrotrillina eocenica, Rotalia trochidoformis, Ranikothalia nuttalli, Lockhartia hunti, Nummulites fabianii, and species of Pellatispira, Linderina, Amphistegina, Heterostegina, Austrotrillina, Calcarina, , Asterocyclina, , Pellistella, Discocyclina, Eorupertia and Operculina. Based mainly on lithofacies and some petrographic samples from different outcrops of the Nisai Formation Kakar et al., (2022) has interpreted deltaic, platform, slope and basinal settings for the Nisai Formation. The type section of the Nisai Formation still lacks detail microfacies studies and in this study we aim to document different microfacies and interpret palaeodepositional setting of the Nisai Formation in the study area.

2. Geological Setting

The Pishin Belt is the northeastern extension of the Makran-Khojak-Pishin Flysch Belt in the northwest of Pakistan. This younger northeast-southwest oriented belt is 700 km long and 200 km wide. The belt is bounded by Eurasian plate (Afghan Block) along strike slip Chaman Fault in the west and northwest and by the Indian Plate along Zhob Valley Thrust in the east-southeast (Lawrence et al., 1981; Bender and Raza, 1995; Jadoon and Khurshid, 1996; Kasi et al., 2012; Ullah et al., 2022, Fig. 1). It is a wide southeast convex belt comprising several thrust-bound stratigraphic zones (Kasi et al., 2012). The Pishin Belt broadly forms a part of the Pishin-Katawaz Basin which was a remnant ocean evolved during the Eocene because of the collision of the Indian and Eurasian plates (Qayyum, 1997; Kasi et al., 2012). The Pishin Belt represents thick sedimentary succession from Eocene to Recent, mostly composed of siliciclastics with some carbonates sediments? Or beds/layers? (Qayyum, 1997; Kasi et al., 2012; Bukhari et al., 2016). The carbonate sediment such as Eocene Nisai Formation is the lower most formation underlying the Muslim Bagh Ophiolite (Kakar et al., 2022). The Oligocene-Early Miocene Khojak Formation, which underlies the Nisai Formation is a fluvio-deltaic and submarine fan succession (Qayyum, 1997; Nizami et al., 2008; Kakar et al., 2016). The Khojak Formation is overlain by the Neogene fluvial successions of the Dasht Murgha Group (Khuzhobai, Bahlol Nika, and Sra Khula, formations), Malthanai and Bostan formations (Kasi et al., 2012, 2017, 2018) (Fig. 1).

3. Methodology

The type section of the Middle-Late Eocene Nisai Formation is exposed at Kazha Mirzai (KM) (N 30°55'49.45" E 68°04'11.80"), Pishin Belt about 12 Km north of Nisai station Killa Saifullah, Pakistan (Fig. 1). The type section of the Nisai Formation was logged and forty-three limestone samples based on lithofacies variation were collected for microfacies analysis (Fig. 2, 3). The limestone samples were made into thin sections, thin sections were studied and photographed using polarizing microscopes in the Centre of Excellence in Mineralogy, University of Balochistan Quetta. Flügel (2010) Comparison chart and Visual estimation method has been utilized to calculate the percentage of various biogenic and abiogenic allochems constituents (Table.1). Five views were taken from each thin section except those which have very low abundance of allochems. Dunham, (1962) classification of carbonate rocks have been used to recognize microfacies, microfacies were given names using low to high abundance of allochems, as microfacies resemble with ramps carbonate.

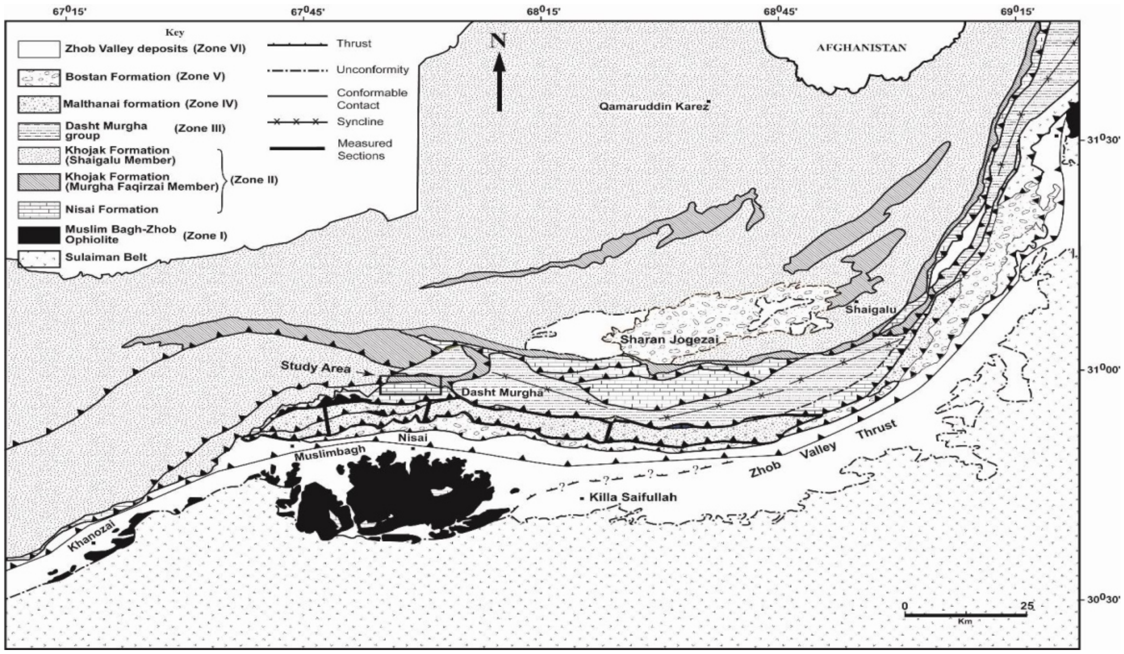

Fig. 1. Generalized lithostratigraphy and tectono-stratigraphic zones of the Pishin Belt, showing the position of study area and surrounding areas (modified after Kasi et al., 2012).

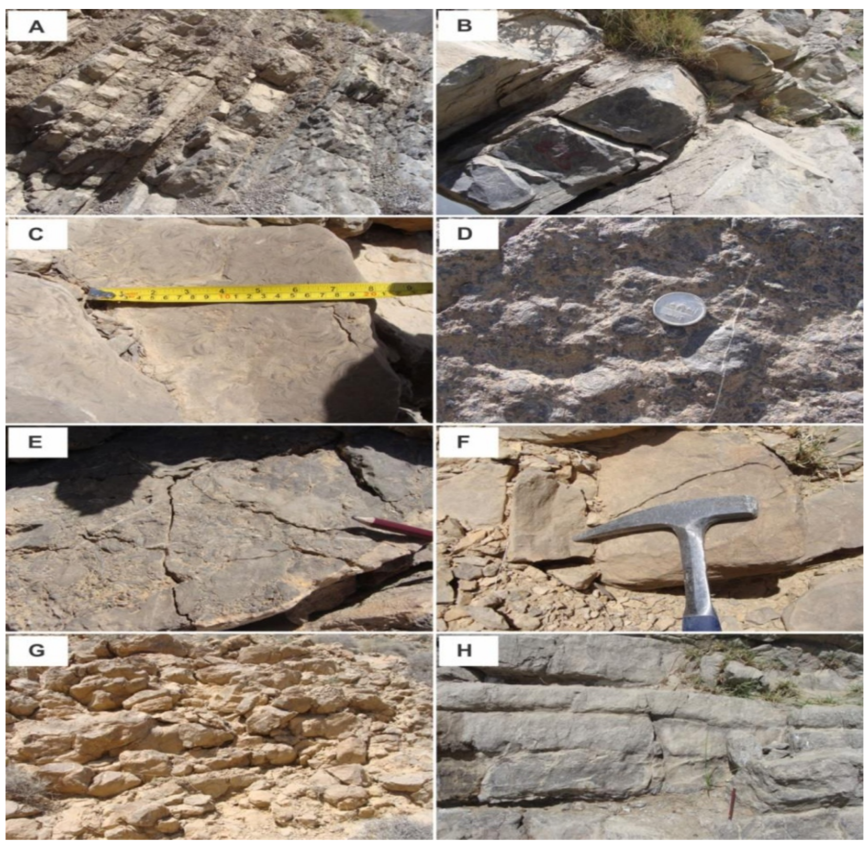

Fig. 2. Field photographs of Nisai Limestone showing the middle unit argillaceous limestone interbedded with shale (A), medium to thick bedded dark grey, argillaceous, limestone in lower part (B), slightly nodular limestone, rich in Discocyclina (C), arenaceous limestone at places, highly fossiliferous, rich in LBF in lowermost unit (D), fossiliferous limestone interbedded with shale present slightly above lowermost part (E), upper part of the section with thick nodular limestone in F), uppermost unit with thick bedded, nodular limestone in G), middle unit with thick, dark grey limestone in H).

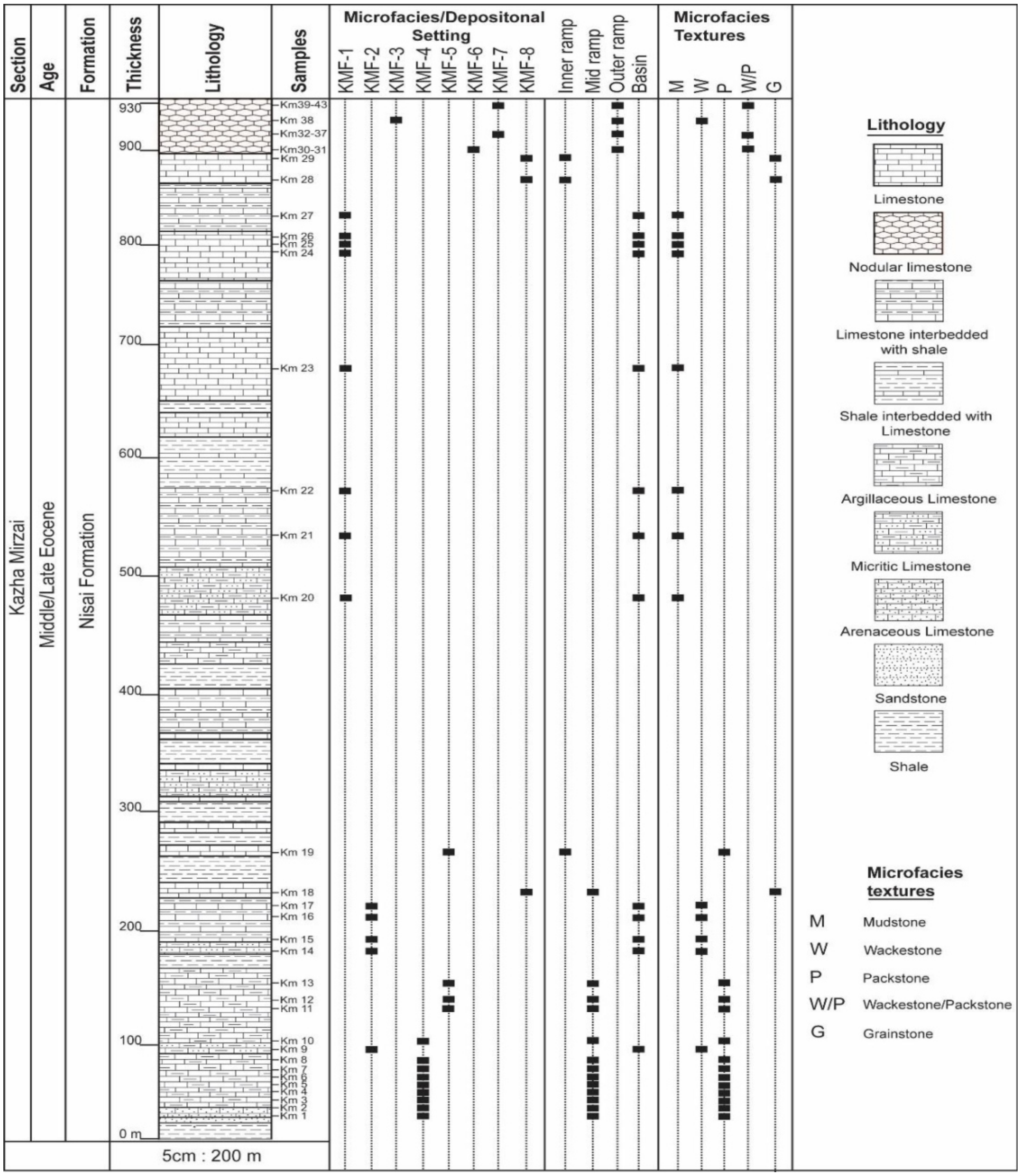

Fig. 3 Lithological column and vertical distribution of microfacies, depositional environment and microfacies textures of the Nisai Formation at the KM section, Pishin Belt, Killa Saifullah.

4. Result and Discussion

4.1. Microfacies of the Nisai Formation at the Type Section Kazha Mirzai (KM)

Petrographic study of the Nisai Formation at KM shows eight major microfacies consisting on mudstone, wackestone, packstone and grainstone. The microfacies are divided into their sub-microfacies based on the allochems content. These are as follows:

- Planktonic Mudstone (KMF-1)
- Planktonic Wackestone (KMF-2)
- Bioclastic LBF Discocyclina Wackestone (KMF-3)
- Siliciclastic Bioclastic LBF Packstone (KMF-4)
- Bioclastic LBF Packstone (KMF-5)
- Bioclastic Planktonic-BF Wackestone-Packstone (KMF-6)
- Bioclastic SBF-LBF Wackestone-Packstone (KMF-7)
- Bioclastic Milliolids Grainstone (KMF-8)

4.1.1 Planktonic Mudstone (KMF-1)

4.1.1.1 Description

In field, this microfacies is represented by thin to medium bedded dark grey argillaceous micrtic limestone interbedded with shale and in the middle unit of section (Fig. 3,2A). This microfacies consist by sample number KM-20 to KM-27. The average allochems are calculated as 9.2%. These skeletal allochems are dominantly planktonic foraminifera (07%), rare bivalves (0.1%), undifferentiated bioclasts (01%) and other foraminifera (1.1%). The remaining 89.8% consists of micrite matrix (Fig. 4, Table.1).

4.1.1.2 Interpretation

The higher percentage of planktonic foraminifera among the skeletal grains and abundance of micritic mud matrix with some bivalves indicate a low energy deep marine condition (Geel, 2000; Flügel, 2010). This facies has been deposited in an open marine condition of distal outer ramp environments, below storm weather base (SWB) and low energy condition suggested for this microfacies (Fig. 3, 12). This microfacies is comparable with the RMF-5 and SMF-3 of the Flügel (2010).

4.1.2 Planktonic Wackestone (KMF-2)

4.1.2.1 Description

In the field this facies is represented by medium to thick-bedded dark grey, argillaceous, limestone, interbedded with shale (Fig. 2B). This microfacies is present in sample number KM-9, KM-14, KM-15 to KM-17. The average allochems are calculated as 26.2%. Allochems mainly consists of skeletal grains (26.2%). The skeletal allochems are dominantly planktonic foraminifera (21%) with some bivalves (1.4%), undifferentiated bioclasts (2.4%) and other foraminifera are (1.4%). The remaining 73.8% constituents is micrite matrix (Fig. 5, Table.1).

4.1.2.2 Interpretation

The rich assemblage of the micritic matrix with the planktonic foraminifers and rare presence of bivalves for this facies suggests outer ramp basinal environment below storm weather base, low energy condition and deepest oligophotic zone (Geel, 2000; Flügel, 2010), which resembles RMF-5 microfacies of Flügel (2010) (Fig. 12).

4.1.3 Bioclastic LBF Discocyclina Wackestone (KMF-3)

4.1.3.1 Description

In the field, this microfacies is represented as medium to thick bedded slightly nodular limestone rich in Discocyclina with some Nummulites and is present in the upper part of the section (Fig. 2C). This facies is represented only by sample KM-38. The microfacies consist of 51% skeletal allochems and 49% micrite matrix. Skeletal allochems dominantly consists of LBF (47%) including Discocyclina (41%), Nummulites (05%), along with algae (01%), brachiopods (01%), undifferentiated bioclasts (02%) and (01%) other foraminifera (Fig. 6, Table.1).

4.1.3.2 Interpretation

Discocyclinas are documented to have occupied outer ramp settings (Gilham and Bristow, 1998; Racey, 1994) but their flattened forms are documented to occur in the mid to outer ramp settings (Loucks et al., 1998) in the lower photic zone in low-Energy water conditions in distal mid to outer ramp settings (Yordanova and Hohenegger, 2002; Beavington-Penney and Racey, 2004; Ćosović et al., 2004; Bassi, 2005). The rich occurrence of Discocyclina along with Nummulites has been interpreted as upper part of the outer ramp for the Eocene carbonates of Italy (Bassi, 2005). The Nummulites are diverse in the mid ramp settings but their ecological range extends to proximal outer ramp settings (Geel, 2000; Payros et al., 2010; Mehar and Adabi, 2014). Here, in our findings this microfacies with micritic matrix with Nummulites, rare brachiopods, algae but dominated by flattened Discocyclina suggests proximal outer ramp settings in a low energy conditions below storm weather wave base and is comparable with the RMF-3 and SMF-8 of the Flügel (2010) (Fig. 3,12).

4.1.4 Siliciclastic Bioclastic LBF Packstone (KMF-4)

4.1.4.1 Description

This facies is present in the lowermost part of the section and is comprised of medium to thick bedded limestone interbedded with shale. The limestone is dark grey, arenaceous at places, highly fossiliferous, rich in LBF (Fig. 2D). The facies is represented by sample KM-1to KM-8 and KM-10). In this microfacies the average allochems are calculated as 50.56%, which mainly consists of skeletal grains (44%), some siliciclasts (3.66%), peloids (2.4%) and extraclasts (0.5%). The skeletal allochems are dominated by larger benthic foraminifera (30.5%) including Nummulites (15.2%), Assilina (09%), Alveolina (0.7%), Discocyclina (2.1%) with some algae (6.3%), echinoderm (2.5%), bryozoans (1.2%), other foraminifera (3.5%) and undifferentiated bioclasts (2.6%). The remaining constituents consist of micrite matrix 45% and sparite cement 4.44% (Fig. 7, Table.1).

4.1.4.2 Interpretation

The diverse assemblages of Assilina represented by species such Assilina leymerie, A. subspinosa, A. laminosa indicate a distal mid ramp environment whereas the diverse and abundant assemblage of Nummulites suggest a middle mid ramp environment (Vaziri-Moghaddam et al., 2006; Adabi et al., 2008; Payros et al., 2010; Mehr and Adabi, 2014; Ishaq et al., 2019; Özgen and Koc-Tasgin, 2019). The co-occurrence of discoidal to lenticular Discocyclinas and coralline red algae has been interpreted as proximal-middle part of the mid ramp (Loucks et al., 1998; Bassi, 2005; Beavington-Penney et al., 2005; Barattolo et al., 2007; Afzal et al., 2011a). The diverse assemblages of Alveolina are common in the distal inner ramp but their ecological range extends to mid ramp (Racey, 2001; Beavington-Penney and Racey, 2004). The presence of brachiopods, echinoderm and bryozoans indicate a shallow marine environment (Scholle and Ulmer-Scholle, 2003).

The presence of quartz grains in the Middle Eocene is related to enhanced continental weathering which was a time of tectonic uplift and warm climate in the region, which caused an increased rainfall on the continental side and contributed siliciclastic to Neo-Tethys Ocean (Kiessling and Kocsis, 2015; Martín-Martín et al., 2020a, 2020b, 2021). The presence of sandstone is more significant in some sections of the Nisai Formation (Kakar et al., 2022).

Hence, the dominant Assilina, Nummulites assemblage, lenticular/discoidal discocyclinas, coralline red algae along with extraclasts, quartz and rare presence inner ramp-derived larger foraminifera such as Alveolina in the micritic matrix indicate high energy condition and turbidity currents. This microfacies suggests a middle-distal mid ramp setting below fair weather wave base (FWWB) in a high energy environment (Fig. 3, 12), and is comparable with RMF 9 of the Flügel (2010).

4.1.5 Bioclastic LB-Foraminifera Packstone (KMF-5)

4.1.5.1 Description

In field, this facies consists of medium to thick bedded fossiliferous limestone interbedded with shale present in the lower part of the formation represented by sample KM-11 to KM-13 and KM-19 (Fig. 2E). The average allochems are calculated as 53.9% and mainly consists of skeletons grains (49.4%) with some extraclasts (1.5%) and peloids (03%). Skeletal allochems include brachiopods (01%), echinoderm (3.5%), bryozoans (02%), algae (3.5%), undifferentiated bioclasts (3.5%) and LBF (35.9%). Foraminifera are rich and diverse represented by Nummulites (17.25%), Assilina (3.7%), Alveolina (1.75 %), milliolids (3.5%), Discocyclina (06%) and some other foraminifera (3.7%). The remaining 46.1% is matrix consisting of 35% micrite matrix and 11.1% is sparite cement (Fig. 8, Table.1).

4.1.5.2 Interpretation

Abundant Nummulites with Assilina are present throughout the mid-ramp setting (Beavington-Penney, 2002, 2004; Beavington-Penney et al., 2006; Vaziri-Moghaddam et al., 2006; Payros et al., 2010; Mehar and Adabi, 2014). Milliolids are common in shallow warm water conditions of inner ramp setting (Geel, 2000; Vaziri-Moghaddam et al., 2006; Brandano et al., 2009) Alveolina indicate a slightly deeper inner ramp environment (Racey, 2001; Beavington-Penney and Racey, 2004). Brachiopods, echinoderm and bryozoans fauna indicate shallow marine condition (Scholle and Ulmer-Scholle, 2003). Coralline red algae with lenticular Discocyclina range in the middle part of the mid ramp (Loucks et al., 1998; Bassi, 2005; Beavington-Penney et al., 2005, 2006; Barattolo et al., 2007; Afzal et al., 2011a).

Hence occurrence of micritic matrix with spirite, rare brachiopods, echinoderms, algae, and diverse assemblage of Nummulites, lenticular Discocyclina, Assilina along with the inner ramp derived Alveolina, milliolids and extraclasts suggests stormy condition of proximal-middle mid-ramp environment below fair weather wave base (FWWB) for this microfacies and is comparable with the SMF-5 and RMF-9 of Flügel, (2010) (Fig. 3, 12).

4.1.6 Bioclastic Planktonic-BF Wackestone-Packstone (KMF-6)

4.1.6.1 Description

This facies is present in the upper part of the section and consists of thick bedded, nodular limestone, represented by sample KM-30 and KM-31 (Fig. 2F). The average allochems calculated in this microfacies are 27%. The skeletal allochems consists of brachiopods (01%), echinoderm (0.5%), bivalves (02%), undifferentiated bioclasts (04%) and foraminifera (19.5%). Foraminifera include Nummulites (3.5%), milliolids (01%), smaller benthic forams (6.5%), Operculina (2.5%) planktonic (05%) and other foraminifera (01%). the remaining 73% constituents' micrite matrix (Fig. 9, Table.1).

4.1.6.2 Interpretation

The presence of smaller benthic indicates outer ramp and upper bathyal settings (Bandy and Arnal, 1960; Zivkovic and Babić, 2003; Martín-Martín et al., 2020a, 2021). Operculina occupies the distal mid ramp to proximal outer ramp 80 m deep photic setting (Sinclair et al., 1998; Hohenegger et al., 2000). Rich micritic matrix with planktonic foraminifera and bivalves are indicating deeper depositional environments likely outer ramp setting (Geel, 2000; Flügel, 2010), with bioclastic re-deposited (mainly fragmented LBFs, echinoderms, brachiopods, and smaller benthic foraminifera are common forms in these settings (Reiss & Hottinger, 1984; Hohenegger and Yordanova, 2001a, 2001b; Ćosović et al., 2004).

Here, the occurrence of smaller benthic, planktonic foraminifera, thin-walled bivalves, micritic matrix with derived upper ramps Operculina, Nummulites, and rare milliolids indicate that outer ramp environment below storm weather base (SWB) is suggested for this microfacies (Flügel, 2010) (Fig. 3, 12).

4.1.7 Bioclastic SBF-LBF Wackestone-Packstone (KMF-7)

4.1.7.1 Description

In field, this facies consists of thick bedded fossiliferous nodular limestone in the uppermost unit of the section and is represented by samples KM-32 to KM-37 and KM-39 to KM-43(Fig. 2G, 3). The average allochems are calculated as 24% which mainly consists of skeletons grains (23.5%) with some peloids (0.5%). Skeletal allochems consists of brachiopods (0.4%), echinoderm (01%), bivalves (01%), undifferentiated bioclasts (03%) and foraminifera (18.1%). Foraminifera include Nummulites (04%), smaller benthic foraminifera (7.9%), Discocyclina (3.2%) milliolids (0.3%) and other foraminifera (03 %). The remaining 76% is micrite matrix (Fig. 10, Table.1).

4.1.7.2 Interpretation

Nummulites association with flattened Discocyclina describes the upper part of the outer ramp oligophotic zone (Bassi, 2005). Small benthic foraminifera range from upper bathyal zone and outer ramp settings (Bandy and Arnal, 1960; Martín-Martín et al., 2020a,b, 2021).

Hence, the occurrence of micritic matrix, brachiopod, echinoderm, bivalves with assemblages of Nummulites, Discocyclina, smaller benthic foraminifera and rare derived milliolids allow interpreting this facies below storm weather base (SWB) in a proximal outer ramp environment and is comparable with the RMF-3 of Flügel, (2010) (Fig. 12).

4.1.8 Bioclastic Milliolids Grainstone (KMF-8)

4.1.8.1 Description

In field, this microfacies are represented by thick bedded, dark grey limestone in the middle unit of the section and is represented by sample KM-18, KM-28 and KM-29 (Fig. 2H). The average allochems are calculated as 33.3%. Allochems mainly consists of skeletal grains (29%), and peloids (4.3%). The skeletal allochems include echinoderm (02%), algae (6.2%), undifferentiated bioclasts (05%) and LBF (15.8%). Foraminifera are dominated by milliolids (12.8%) with some other foraminifera (03%). The remaining 66.7% is the sparite cement (Fig. 11, Table.1).

4.1.8.2 Interpretation

Milliolids indicate shallow warm water environment of inner ramp condition (Geel, 2000; Vaziri-Moghaddam et al., 2006; Brandano et al., 2009) and the association of echinoderm and algae with milliolids supports shallow marine settings (Scholle and Ulmer-Scholle, 2003).

Hence, the association of milliolids, echinoderms, algae and the presence of abundant spar cement suggests stormy condition of inner ramp environment which is comparable with the RMF 27 of Flügel, (2010) (Fig. 12).

4.2 Depositional model

The rich biogenic components, dominant micritic matrix with sparite at places, vertically strong facies variation, association of different faunal groups and algae, and the inferred paleodepositional environment for each microfacies of the Nisai Formation suggests overall deposition in an inner ramp to basinal distal outer ramp environment (Fig. 12). In this study the distribution of algae, planktonic foraminifera, different types of LBF, other skeletal grains, matrix types and their ratio to skeletal grains are utilized to interpret the depositional setting of these Eocene limestones. The diagnostic characteristic of foraminifera such as test size and shape (flattened, lenticular/discoidal) are excellent indicators of their palaeodepositional environment (Rasser et al., 2005; Hallock and Glenn, 1986).

The most dominant groups among larger benthic foraminfera in Eocene are orthophragminids (Discocyclina, Asterocyclina) nummulitids, alveolinids and miliolids (Hottinger, 1997; Geel, 2000; Racey, 2001; Mehr and Adabi, 2014; Pomar et al., 2017). The biodiversity and abundance of each individual group indicates a specific depth and environment. Dicocyclinids are common in the mid ramp to proximal outer ramp settings. The lenticular discocyclinds are most common in the mesophotic mid ramp setting whereas the flattened forms occupied deep water of the proximal outer ramp environment down to lower photic zone where the LBF biodiversity is mainly restricted to flattened discocyclinids (Zamagni et al., 2008; Beavington-Penney and Racey, 2004; Afzal et al., 2011a). The nummulitids (Assilina and Nummulites) are abundant in the mesophotic mid-ramp environments and the alveolinids and milliolids are more diverse in the inner ramp Euphotic Zone (Racey, 1994; Bassi, 2005; Barattolo et al., 2007; Adabi et al., 2008; Afzal et al., 2011) (Fig. 3, 12). Red algae are generally considered mesophotic mid ramp biota (Pomar et al., 2017). The deposition is arranged in a deepening sequence that ends with planktic foramifer-rich calcareous marls (Báldi-Beke and Báldi, 1991; Kázmér et al., 2003).

Thus, the LBF are important tools to model paleoenvironments in shallow-marine settings (Geel, 2000; Racey, 2001) and used as excellent indicators for facies interpretation (Rasser et al., 2005; Mehr and Adabi, 2014). The LBF and algae were significant carbonate producers in shallow-marine ramp setting during Eocene time across the world (Racey, 2001; Wilson and Vecsei, 2005; Pay-ros et al., 2010).

Table 1. Show petrographical visually estimated average allochems constituents of microfacies in Nisai Formation, Kazha Mirzai section, Killa Saifullah.

Facies	Siliciclasts %	Peloids %	Extraclasts %	Bioclasts % — Foraminifera: Nummulites %	Assilina %	Alveolina %	Milliolids %	Smaller-Benthic-Forams %	Discocyclina %	Plankton %	Operculina %	Other forams %	Other Flora and Fauna: Algae %	Brachiopods %	Echinoderms %	Bryozoans %	Bivalves %	Undifferentiated Bioclasts %	Average Allochems %	Micrite Matrix %	Sparite Matrix %
KMF-1	–	–	–	–	–	–	–	–	–	07	–	1.1	–	–	–	–	0.1	1.1	9.2	89.8	–
KMF-2	–	–	–	–	–	–	–	–	–	21	–	1.4	–	–	–	–	1.4	2.4	24.2	73.8	–
KMF-3	–	–	–	05	–	–	–	–	41	–	–	01	01	01	–	–	–	02	51	49	–
KMF-4	3.66	2.4	0.5	15.2	09	0.7	–	–	2.1	–	–	3.5	6.3	–	2.5	1.2	–	2.6	50.56	45	4.44
KMF-5	–	03	1.5	17.25	3.7	1.75	3.5	–	06	–	–	3.7	3.5	01	3.5	02	–	3.5	53.9	35	11.1
KMF-6	–	–	–	3.5	–	–	01	6.5	–	05	2.5	01	–	01	0.5	–	02	04	27	73	–
KMF-7	–	0.5	–	04	–	–	0.3	7.9	3.2	–	–	0.3	–	0.4	01	–	01	03	24	76	–
KMF-8	–	4.3	–	–	–	–	12.8	–	–	–	–	03	6.2	–	02	–	–	05	33.3	–	66.7

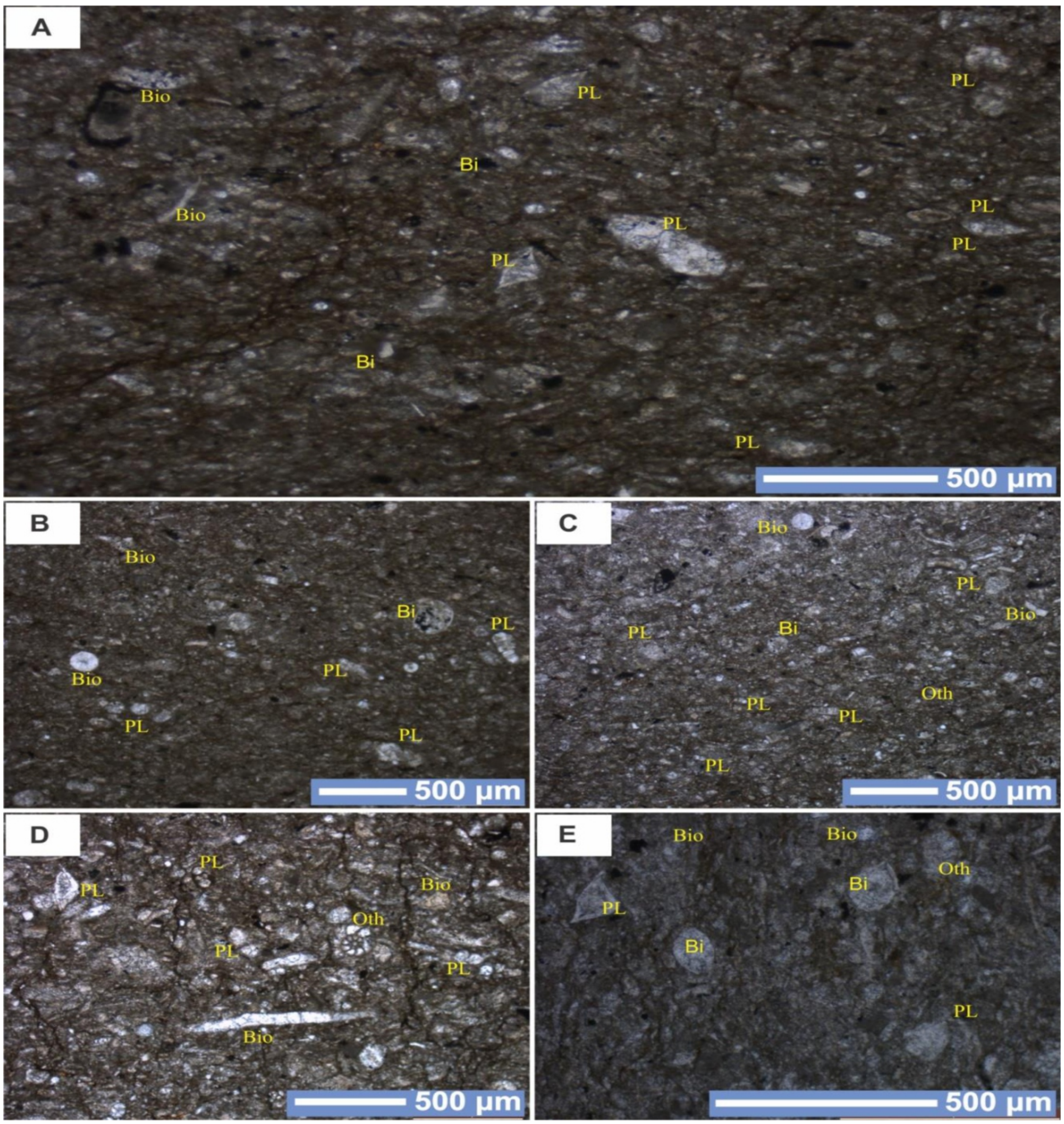

Fig. 4 photomicrographs of the Planktonic Mudstone Microfacies showing planktonic foraminifera (PL in A to E), bivalves (Bi in A to C and E), other foraminifera (Oth) in C, D and E), and undifferentiated bioclasts (Bio) in A to E).

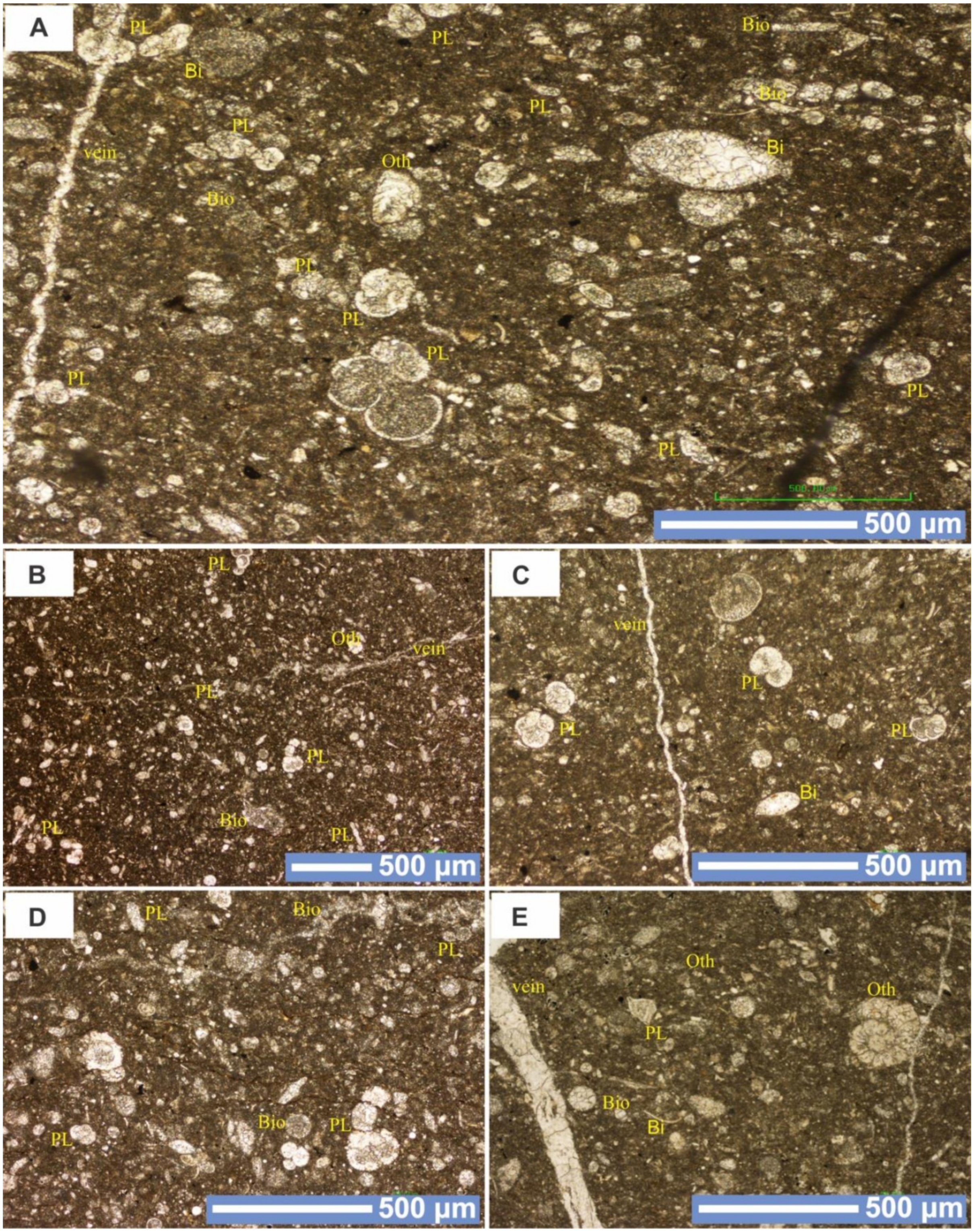

Fig. 5 photomicrographs of the Planktonic Wackestone Microfacies showing planktonic foraminifera (PL in A to E), bivalves (Bi in A, C and E), other foraminifera (Oth) in A, B, D, E), and undifferentiated bioclasts (Bio) in A to E).

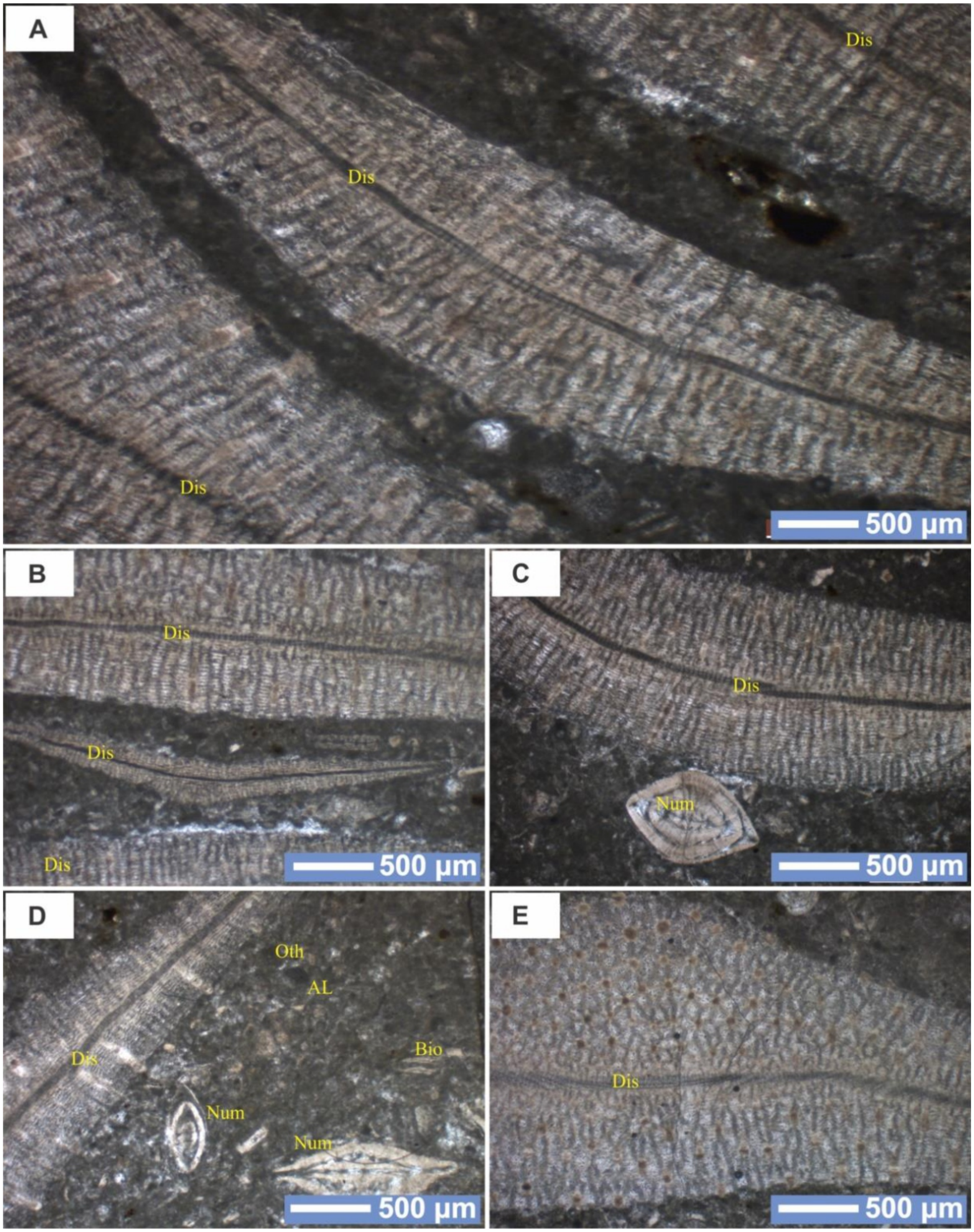

Fig. 6 photomicrographs of Bioclastic LBF Discocyclina Wackestone Microfacies showing Discocyclina (Dis) in A to E), Nummulites (Num) in C, D), other foraminifera (Oth) in D), algae (Al) in D), and undifferentiated bioclasts (Bio) in D).

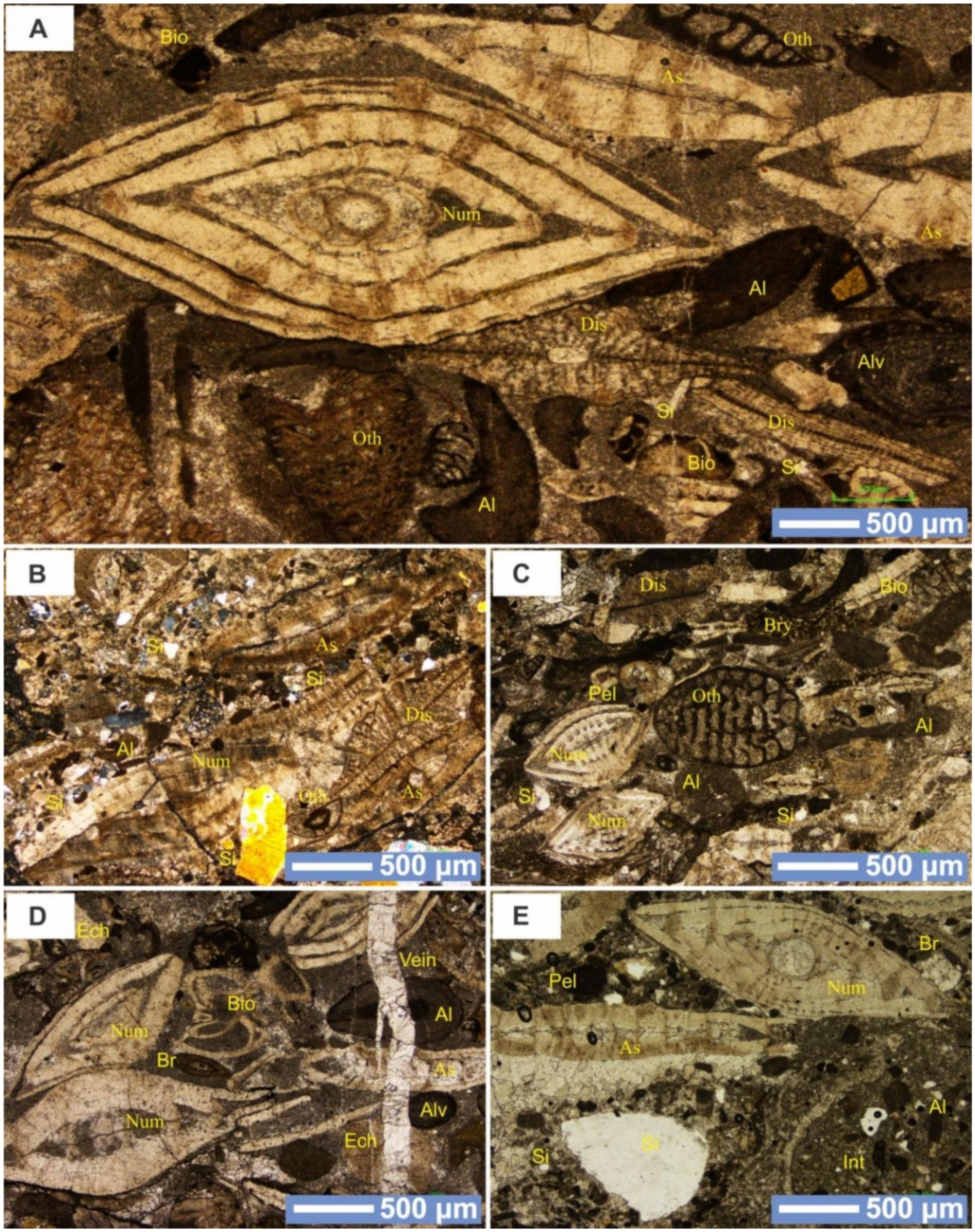

Fig. 7 photomicrographs of Siliciclastic Bioclastic LBF Packstone Microfacies showing the Nummulites (Num) in A to E), Assilina (As) in A, B, D and E), Discocyclina (Dis) in A to C), Alveolina (Alv A in D), other foraminifera (Oth in A, to C), brachiopods (Br in D and E), echinoderm (Ech) in D), bryozoans (Bry) in C), siliciclasts (Si) in A to E), extraclasts (Ext) in E), peloids (Pel) in C, E), algae (Al) in A to E), calcite vein (Vein) in D), and undifferentiated bioclasts (Bio) in A, C and D).

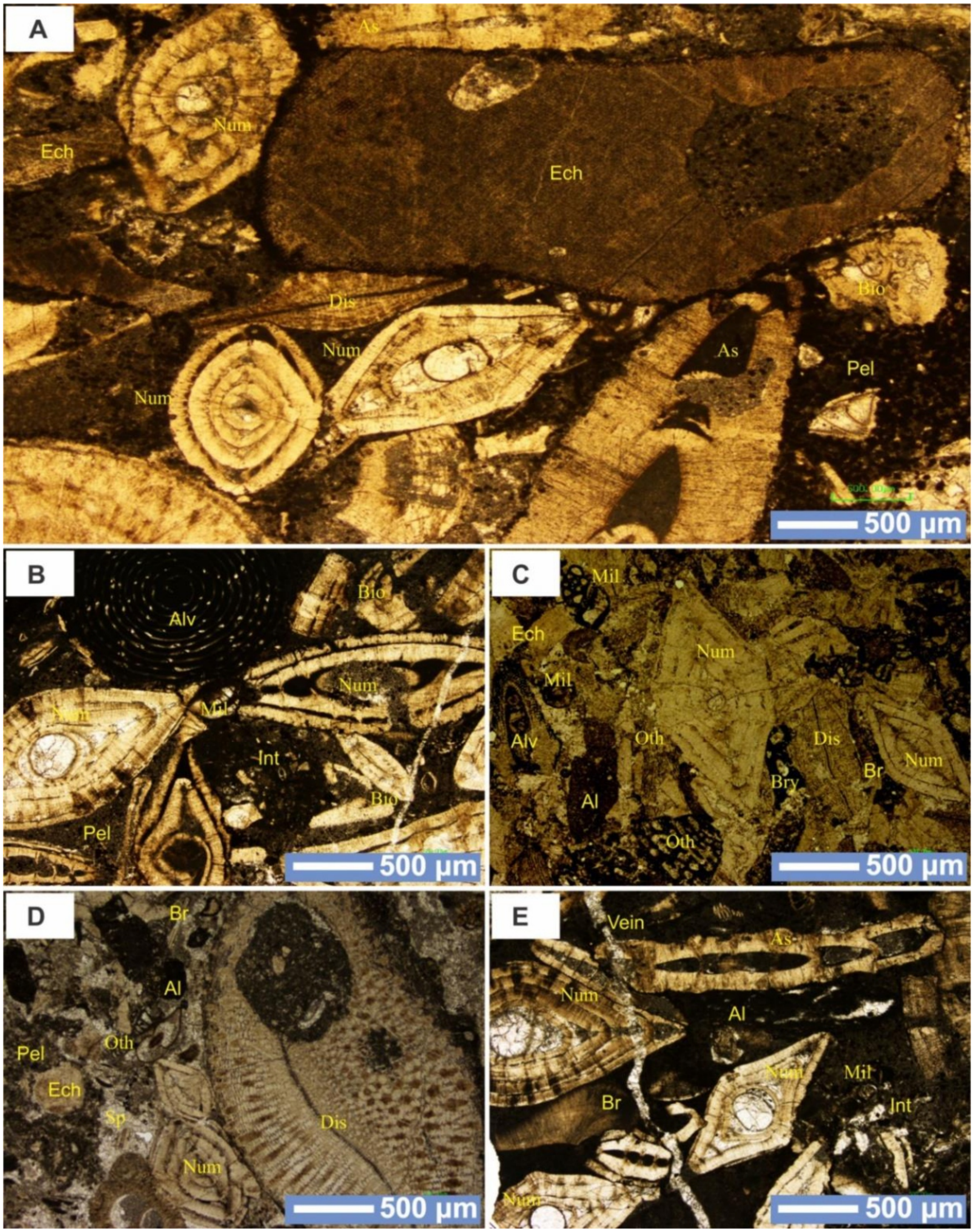

Fig. 8 photomicrographs of Bioclastic LB-Foraminifera Packstone Microfacies showing Nummulites (Num) in A to E), Assilina (As) in A and E), Discocyclina (Dis) in A, C and D), Alveolina (Alv in B), milliolids (Mil in B, C and E), other foraminifera (Oth) in C and D), brachiopods (Br in C to E), echinoderm (Ech in A, C and D), bryozoans (Bry in C), extraclasts (Ext in B and E), peloids (Pel in A, B and D), algae (Al in C to E), calcite vein (Vein in E), spar (Sp) in D) and undifferentiated bioclasts (Bio) in A and B).

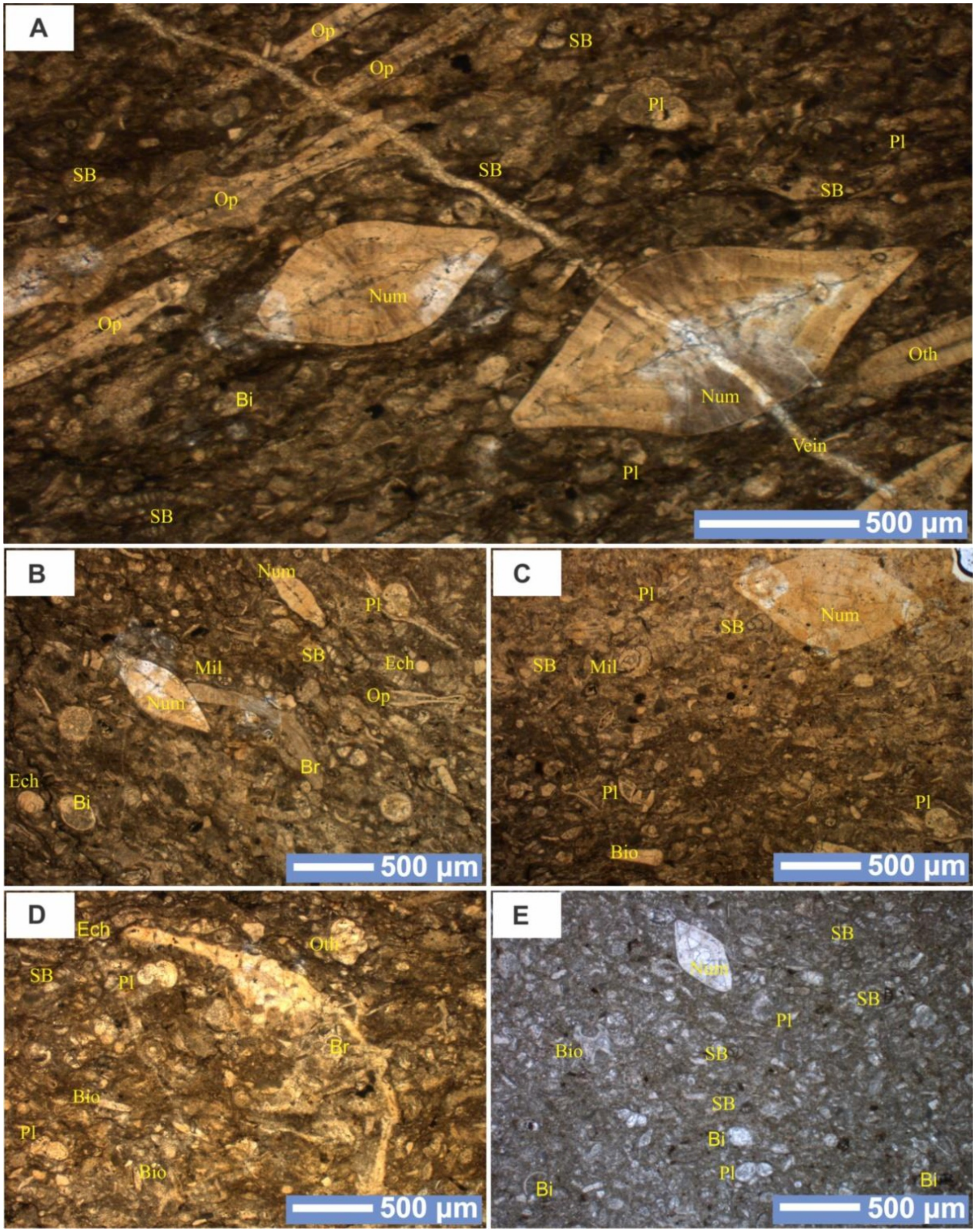

Fig. 9 photomicrographs of Bioclastic Planktonic-BF Wackestone-Packstone Microfacies showing the Planktonic foraminifera (PL in A to E) Nummulites (Num) in A to C and E), smaller benthic foraminifera (SB) in A to E), Operculina (Op in A and B), milliolids (Mil) in B and C), other foraminifera (Oth) in A), brachiopods (Br) in B and D), echinoderm (Ech) in B and D), bivalves (Bi) in A, B and E) and calcite vein (Vein in A), and undifferentiated bioclasts (Bio) in C to E).

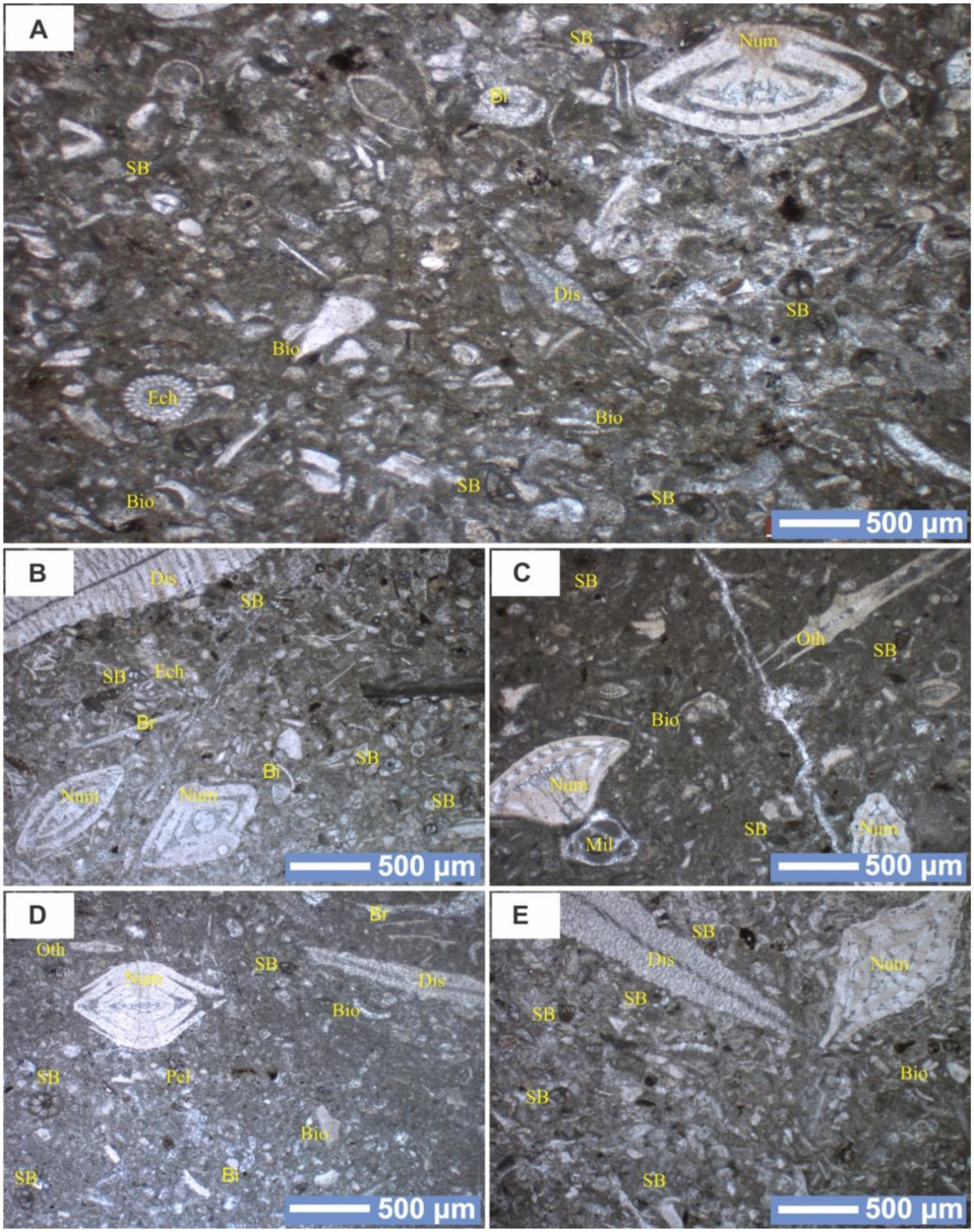

Fig. 10 photomicrographs of Bioclastic SBF-LBF Wackestone-Packstone Microfacies showing smaller benthic foraminifera (SB in to E), Nummulites (Num in A to E), Disscocyclina (Dis) in A, B, D and E), milliolids (Mil in C), other foraminifera (Oth) in B and C), brachiopods (Br) in B and D), echinoderm (Ech) in A and B), bivalves (Bi in A, B and D) peloids (Pel) in D), and undifferentiated bioclasts (Bio in A and C to E).

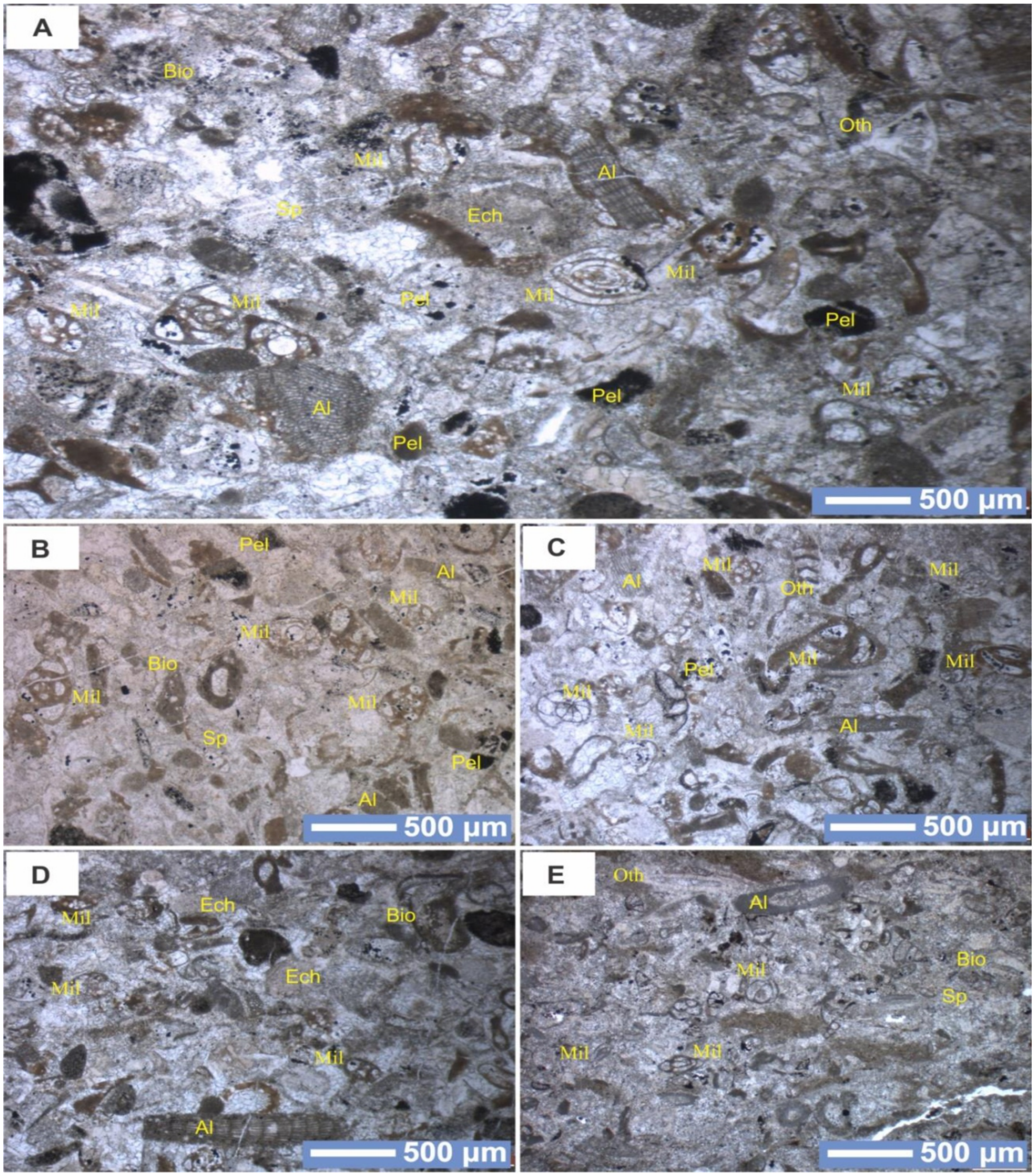

Fig. 11 photomicrographs of Bioclastic Milliolids Grainstone Microfacies showing milliolids (Mil) in A to E), other foraminifera (Oth) in A, C, E), echinoderm (Ech) in A, D), peloids (Pel in A and B), algae (Al in A to E), and undifferentiated bioclasts (Bio in A, B, D and E).

Eight microfacies identified in the Nisai Formation dominantly consists of LBF, with some algae, smaller benthic foraminifera, planktonic foraminifera and some other biogenic components such as brachiopods, molluscs and bryozoans. The KMF-8 facies with dominant milliolids indicates an inner ramp setting whereas the KMF 4 and KMF 5 are dominated by Nummulites, Assilina, and lenticular Discocyclina with some siliciclastic input indicates that these facies have been deposited in a mid-ramp setting. The presence of siliciclastic hints towards active tectonics in the region as the uplifting was taking place and may have caused an enhanced continental weathering which is noticed in other sections of the Nisai Formation in the form of thick sandstone beds in the Nisai Formation (Kakar et al., 2022). During the Eocene time as the The KMF-3 is dominated by flattened Discocyclina indicating an outer ramp setting. KMF-1-2 the planktonic foraminifera are found as mudstones and wackestone with some smaller benthic foraminifera at places indicating a deep basinal setting. The existence of LBF in the Nisai Formation of Pishin Basin reflects that the deposition of this formation has taken place during the persistence of tropical-subtropical climate as compared to other carbonate ramps of Tethys (Buxton and Pedley, 1989). On the basis of established microfacies of limestones of the Nisai Formation the homoclinal slope foraminifer's dominant carbonate ramp is suggested for this formation. The ramp setting for Nisai Formation is supported by the lack of reef building organism, the greater quantities of micrite in almost every microfacies, lack of redeposition, rareness of grainstone microfacies, and gentle inclination of shallow platform to basin (Wright, 1986; Mehr and Adabi, 2014).

According to Racey, (1994) and Gilham and Bristow, (1998) ramp models, the Nisai Limestone can be divided into inner, middle and outer ramp. The inner ramp settings are rich in milliolids and alveolinids microfacies, while the mid ramp microfacies are rich in lenticular Discocyclina and nummulitids. The interpreted environments and their vertical variations demonstrate that the deposition has taken place as asymmetric cyclic, reflecting that most of the limestone has been formed in regression.

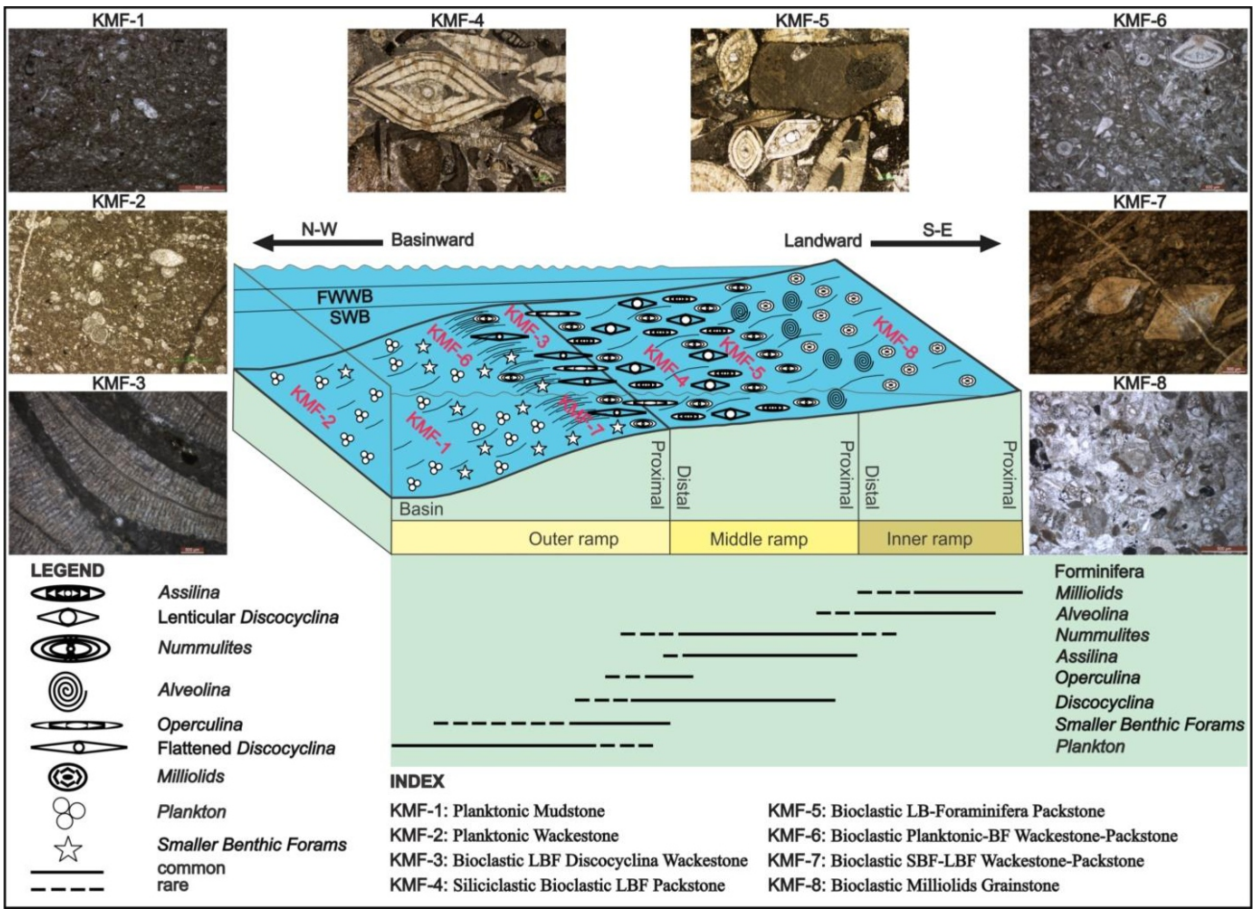

Fig. 12 Suggested depositional model of the Nisai Formation for the Kazha Mirzai section (modified after Flügel, 2010), and distributions scheme of benthic and planktonic foraminifera along the ramp (after Gilham and Bristow, 1998; Geel, 2000; Beavington-Penney and Racey, 2004).

5. Conclusions

The Nisai Formation in the study area is 930 m thick and is composed of thick, medium and thin bedded and nodular limestone with olive greenish grey shale. The Nisai Formation in the type section is rich in fossils at places and the microfacies analysis reveal eight different microfacies types. These microfacies contain various skeletal allochems such as LBF, small foraminifera, planktonic foraminifera, red algae, bryozoan and brachiopods. Six of these microfacies are abundant with allochems of LBF which include assemblages of Nummulites, Assilina, Discocyclina, Alveolina and milliolids with rare smaller benthic foraminifera at places whereas two facies contain planktonic foraminifera embedded in mudstone to wackestone. These microfacies of Nisai Formation are Planktonic Mudstone (KMF-1), Planktonic Wackestone (KMF-2), Bioclastic LBF Discocyclina Wackestone (KMF-3), Siliciclastic Bioclastic LBF Packstone (KMF-4), Bioclastic LBF Packstone (KMF-5), Bioclastic Planktonic-BF Wackestone-Packstone (KMF-6), Bioclastic SBF-LBF Wackestone-Packstone (KMF-7), Bioclastic Milliolids Grainstone (KMF-8) and their identified environment of deposition suggests that the Nisai Formation in the study area has been deposited in an inner ramp to outer ramp basinal settings.

Acknowledgement

We thank Centre of Excellence in Mineralogy, University of Balochistan, Quetta for supporting this study. We are grateful to Dr Tian Jiang (China University of Geosciences, Beijing) and the unknown reviewer for their constructive reviews on this paper.

Authors' Contribution

Abdullah was leading the whole study, and was involved in fieldwork, lab analysis and write up. Mohibullah and Aimal Khan Kasi proposed the main concept and were involved in field data collection and write up. Shams ul Alam, assisted in establishing microfacies of the section. Ejaz ul Haq, contributed in making figures and was also involved in write up.

References

Adabi, M.H., Zohdi, A., Ghabeishavi, A., Amiri-Bakhtiyar, H., 2008. Applications of nummulitids and other larger benthic foraminifera in depositional environment and sequence stratigraphy: an example from the Eocene deposits in Zagros Basin, SW Iran. Facies, 54, 499-512.

Afzal, J., Williams, M., Aldridge, R.J., 2009. Revised stratigraphy of the lower Cenozoic succession of the Greater Indus Basin in Pakistan. Journal of Micropalaeontology, 28, 7-23.

Afzal, J., Williams, M., Leng, M.J., Aldridge, R.J., 2011a. Dynamic response of the shallow marine benthic ecosystem to regional and pan-Tethyan environmental change at the Paleocene–Eocene boundary. Palaeogeography, Palaeoclimatology, Palaeoecology, 309, 141-160.

Afzal, J., Williams, M., Leng, M.J., Aldridge, R.J., Stephenson, M.H., 2011b. Evolution of Paleocene to Early Eocene larger benthic foraminifer assemblages of the Indus Basin, Pakistan. Lethaia, 44, 299-320.

Babar, N., Mohibullah, M., Kasi, A.K., Ali, N., Khan, A., 2018. Foraminiferal Biostratigraphy of the Eocene Kirthar Formation, western Sulaiman Fold-Thrust Belt, Balochistan, Pakistan. Journal of Himalayan Earth Science, 51.

Báldi-Beke, M., Báldi, T., 1991. Palaeobathymetry and palaeogeography of the Bakony Eocene Basin in western Hungary. Palaeogeography, Palaeoclimatology, Palaeoecology, 88(1-2), 25-52.

Bandy, O., L., Arnal, R.E., 1960. Concepts of foraminiferal paleoecology. AAPG bulletin, 44, 1921-1932.

Barattolo, F., Bassi, D., Romano, R., 2007. Upper Eocene larger foraminiferal–coralline algal facies from the Klokova Mountain (southern continental Greece). Facies, 53, 361-375.

Bassi, D., 2005. Larger foraminiferal and coralline algal facies in an Upper Eocene storm-influenced, shallow-water carbonate platform (Colli Berici, north-eastern Italy). Palaeogeography, Palaeoclimatology, Palaeoecology, 226, 17-35.

Beavington-Penney, S.J., 2002. Characterisation of selected Eocene Nummulites accumulations (Doctoral dissertation, CARDIFF).

Beavington-Penney, S.J., 2004. Analysis of the effects of abrasion on the test of Palaeonummulites venosus: implications for the origin of nummulithoclastic sediments. Palaios, 19, 143-155.

Beavington-Penney, S.J., Paul Wright, V., Racey, A., 2005. Sediment production and dispersal on foraminifera-dominated early Tertiary ramps: the Eocene El Garia Formation, Tunisia. Sedimentology, 52, 537-569.

Beavington-Penney, S.J., Racey, A., 2004. Ecology of extant nummulitids and other larger benthic foraminifera: applications in palaeoenvironmental analysis. Earth-Science Reviews, 67, 219-265.

Beavington-Penney, S.J., Wright, V.P., Racey, A., 2006. The middle Eocene Seeb Formation of Oman: an investigation of acyclicity, stratigraphic completeness, and accumulation rates in shallow marine carbonate settings. Journal of Sedimentary Research, 76, 1137-1161.

Bender, F.K., Bender, F.K., Raza, H.A., 1995. Paleographic and geodynamic evolution. In Geology of Pakistan pp. 162-118, Berlin: Gebruder Borntraeger.

Brandano, M., Frezza, V., Tomassetti, L., Cuffaro, M., 2009. Heterozoan carbonates in oligotrophic tropical waters: the Attard member of the lower coralline limestone formation (Upper Oligocene, Malta). Palaeogeography, Palaeoclimatology, Palaeoecology, 274, 54-63.

Bukhari, S.W.H., Mohibullah, M., Kasi, A.K., Iqbal, H., 2016. Biostratigraphy of the Eocene Nisai Formation in Pishin Belt, Western Pakistan. Journal of Himalayan Earth Sciences, 49, 17.

Buxton, M.W., N., Pedley, H.M., 1989. Short Paper: A standardized model for Tethyan Tertiary carbonate ramps. Journal of the Geological Society, 146, 746-748.

Ćosović, V., Drobne, K., Moro, A., 2004. Paleoenvironmental model for Eocene foraminiferal limestones of the Adriatic carbonate platform (Istrian Peninsula). Facies, 50, 61-75.

Dunham, R.J., 1962. Classifcation of carbonate rocks according to depositional texture. In: Ham WE (ed) Classifcation of car-bonate rocks. Memoir American Association of Petroleum Geologists, vol 1, pp 108–121

Flügel, E., 2010. Microfacies of carbonate rocks: analysis, interpretation and application, 2nd edn. Springer, Berlin. https ://doi.org/10.1007/978-3-642-03796-2

Geel, T., 2000. Recognition of stratigraphic sequences in carbonate platform and slope deposits: empirical models based on microfacies analysis of Palaeogene deposits in southeastern Spain. Palaeogeography, Palaeoclimatology, Palaeoecology, 155, 211-238.

Gilham, R.F., Bristow, C.S., 1998. Facies architecture and geometry of a prograding carbonate ramp during the early stages of foreland basin evolution: lower Eocene sequences, Sierra del Cadí, SE Pyrenees, Spain. Geological Society, London, Special Publications, 149, 181-203.

Hallock, P., 2001. Coral reefs, carbonate sediments, nutrients, and global change. In The history and sedimentology of ancient reef systems (pp. 387-427). Springer, Boston, MA.

Hallock, P., Glenn, E.C., 1986. Larger foraminifera: a tool for paleoenvironmental analysis of Cenozoic carbonate depositional facies. Palaios, 55-64.

Hanif, M., Hart, M.B., Grimes, S.T., Leng, M.J., 2014. Integrated stratigraphy and palaeoenvironment of the P/E boundary interval, Rakhi Nala section, Indus Basin (Pakistan). Arabian Journal of Geosciences, 7, 323-339.

Hohenegger, J., Yordanova, E., 2001a. Depth–transport functions and erosion–deposition diagrams as indicators of slope inclination and time-averaged traction forces: applications in tropical reef environments. Sedimentology, 48, 1025-1046.

Hohenegger, J., Yordanova, E., 2001b. Displacement of larger foraminifera at the western slope of Motobu Peninsula (Okinawa, Japan). Palaios, 16, 53-72.

Hohenegger, J., Yordanova, E., Hatta, A., 2000. Remarks on west Pacific Nummulitidae (foraminifera). The Journal of Foraminiferal Research, 30, 3-28.

Hottinger, L., 1997. Shallow benthic

foraminiferal assemblages as signals for depth of their deposition and their limitations. Bulletin de la Société géologique de France, 168, 491-505.

Hottinger, L., 1998. Shallow benthic foraminifera at the Paleocene-Eocene boundary. Verlag nicht ermittelbar strata serie 1, 9, 6-64.

Ishaq, M., Jan, I.U., Hanif, M., Awais, M., 2019. Microfacies and diagenetic studies of the early Eocene Sakesar Limestone, Potwar Plateau, Pakistan: approach of reservoir evaluation using outcrop analogue. Carbonates and Evaporites 34, 623–656.

Jadoon, I.A., Khurshid, A., 1996. Gravity and tectonic model across the Sulaiman fold belt and the Chaman fault zone in western Pakistan and eastern Afghanistan. Tectonophysics, 254, 89-109.

Kakar, A., Kasi, A.M., Benedetti, A., Kasi, A.K., 2022. Stratigraphy and depositional environment of a mixed siliciclastic-carbonate platform and slope succession of the Paleogene Nisai Group, Pakistan. STRATIGRAPHY, 19, 95-117.

Kakar, D.M., Kasi, A.K., Kassi, A.M., Friis, H., Mohibullah, M., Khan, S., 2016. Petrography and Whole-Rock Geochemistry of the Oligocene-Miocene Khojak Formation Khojak-Pishin Belt, Pakistan: Implications on Provenance and Source Area Weathering. Journal of Himalayan Earth Science, 49 (2), 135-157.

Kamran, M., Frontalini, F., Xi, D., Papazzoni, C.A., Jafarian, A., Latif, K., Wan, X., 2021. Larger benthic foraminiferal response to the PETM in the Potwar Basin (Eastern Neotethys, Pakistan). Palaeogeography, Palaeoclimatology, Palaeoecology, 575, 110450.

Kasi, A.K., Kassi, A.M., Friis, H., Manan, R.A., 2017. Petrology and provenance of the Neogene fluvial succession in Pishin Belt (Katawaz Basin) western Pakistan: implications for sedimentation in peripheral forelands basins. Geosciences Journal, 21, 149-166.

Kasi, A.K., Kassi, A.M., Umar, M., Friis, H., Mohibullah, M., Manan, R.A., 2018. A Paleogeographic and Depositional Model for the Neogene Fluvial Succession, Pishin Belt, Northwest Pakistan: Effect of Post Collisional Tectonics on Sedimentation in a Peripheral Foreland Setting. Acta Geologica Sinica, 92(2), 499-518.

Kasi, A.K., Kassi, A.M., Umar, M., Manan, R.A., Kakar, M.I., 2012. Revised lithostratigraphy of the Pishin Belt, northwestern Pakistan. Journal of Himalayan Earth Science, 45(1).

Kázmér, M., Dunkl, I., Frisch, W., Kuhlemann, J., Ozsvárt, P., 2003. The Palaeogene forearc basin of the Eastern Alps and Western Carpathians: subduction erosion and basin evolution. Journal of the Geological society, 160, 413-428.

Kiessling, W., Kocsis, Á.T., 2015. Biodiversity dynamics and environmental occupancy of fossil azooxanthellate and zooxanthellate scleractinian corals. Paleobiology, 41, 402-414.

Lawrence, R.D., Yeats, R.S., Khan, S.H., Farah, A., DeJong, K.A., 1981. Thrust and strike slip fault interaction along the Chaman transform zone, Pakistan. Geological Society, London, Special Publications, 9(1), 363-370.

Loucks, R.G., Moody, R.T., J., Bellis, J.K., Brown, A.A., 1998. Regional depositional setting and pore network systems of the El Garia Formation (Metlaoui Group, Lower Eocene), offshore Tunisia. Geological Society, London, Special Publications, 132, 355-374.

Martín-Martín, M., Guerrera, F., Miclăuș, C., Tramontana, M., 2020b. Similar Oligo-Miocene tectono-sedimentary evolution of the Paratethyan branches represented by the Moldavidian Basin and Maghrebian Flysch Basin. Sedimentary Geology, 396, 105548.

Martín-Martín, M., Guerrera, F., Tosquella, J., Tramontana, M., 2021. Middle Eocene carbonate platforms of the westernmost Tethys. Sedimentary Geology, 415, 105861.

Martín-Martín, M., Guerrera, F., Tosquella, J., Tramontana, M., 2020a. Paleocene-Lower Eocene carbonate platforms of westernmost Tethys. Sedimentary geology, 404, 105674.

Mehr M.K., Adabi M.H., 2014. Microfacies and geochemical evidence for original aragonite mineralogy of a foraminifera-dominated carbonate ramp system in the late Paleocene to Middle Eocene, Alborz basin, Iran. Carbonates Evaporites, 29:155–175.

Nizami, A.R., Ashraf, M., Mahmood, M.N., Imran, M., Randhawa, A.S., Rafique, M.I., 2008. Diagenetic Sequence and Microfacies Assemblages of the Upper Eocene Nisai Formation, Pishin Basin, Balochistan, Pakistan. Geological Bulletin Punjab University, 43, 35-48.

Özgen-Erdem, N., Koç-Tasgin, C., 2019. Microfacies and depositional environment of the ilerdian carbonates in the North-Western Tosya (SE Kastamonu) region, Northern Turkey. Journal of the Geological Society of India, 93, 704-712.

Payros, A., Pujalte, V., Tosquella, J., Orue-Etxebarria, X., 2010. The Eocene storm-dominated foralgal ramp of the western Pyrenees (Urbasa–Andia Formation): an analogue of future shallow-marine carbonate systems. Sedimentary Geology, 228, 184-204.

Pomar, L., Baceta, J.I., Hallock, P., Mateu-Vicens, G., Basso, D., 2017. Reef building and carbonate production modes in the west-central Tethys during the Cenozoic. Marine and Petroleum Geology, 83, 261-304.

Pomar, L., Hallock, P., 2008. Carbonate factories: a conundrum in sedimentary geology. Earth-Science Reviews, 87, 134-169.

Qayyum, M., Lawrence, R.D., Niem, A.R., 1997. Molasse-delta-flysch continuum of the Himalayan orogeny and closure of the Paleogene Katawaz remnant ocean, Pakistan. International geology review, 39, 861-875.

Racey A., (1994). Biostratigraphy and palaeobiogeographic signifcance of Tertiary nummulitids (Foraminifera) from northern Oman. In: Simmons MD (ed) Micropalaeontology and hydrocarbon exploration in the Middle East. Chapman and Hall, London, pp, 343–370.

Racey, A., 2001. A review of Eocene nummulite accumulations: structure, formation and reservoir potential. Journal of petroleum geology, 24, 79-100.

Rasser, M.W., Scheibner, C., Mutti, M., 2005. A paleoenvironmental standard section for Early Ilerdian tropical carbonate factories (Corbieres, France; Pyrenees, Spain). Facies, 51, 218-232.

Rehman, H., Mohibullah, M., Kasi, A.K., Hussain, H.S., 2018. Foraminiferal biostratigraphy of the Dungan Formation, Harnai area, western Sulaiman Fold-Thrust Belt Pakistan. Journal Of Himalayan Earth Sciences, 51, 34–43.

Reiss, Z., Hottinger, L., 1984. Shell producers in the water column. In The Gulf of Aqaba, Springer, Berlin, Heidelberg, pp, 89-138.

Scheibner, C., Speijer, R.P., 2008. Late Paleocene-early Eocene Tethyan carbonates platform evolution-A response to long-and short-term paleoclimatic change. Earth-Science Reviews, 90, 71-102.

Scholle, P.A., Ulmer-Scholle, D.S., 2003. A color guide to the petrography of carbonate rocks: grains, textures, porosity, diagenesis, AAPG Memoir 77 (Vol. 77). AAPG.

Sinclair, H.D., Sayer, Z.R., Tucker, M.E., 1998. Carbonate sedimentation during early foreland basin subsidence: the Eocene succession of the French Alps. Geological Society, London, Special Publications, 149, 205-227.

Uddin, N., Babar, N., Mohibullah, M., Kasi, A.K., Khan, M., Ghani, M., 2019. Biostratigraphy of the Kirthar formation, Mach area, Sulaiman fold-Thrust Belt, Balochistan, Pakistan. Bahria University Research Journal of Earth Sciences, 4, 1-6.

Ullah, S., Jan, I. U., Hanif, M., Latif, K., Mohibullah, M., Sabba, M., ... & Vo Thanh, H. (2022). Paleoenvironmental and bio-sequence stratigraphic analysis of the cretaceous pelagic carbonates of eastern tethys, sulaiman range, Pakistan. Minerals, 12(8), 946.

Vaziri-Moghaddam, H., Kimiagari, M., Taheri, A., 2006. Depositional environment and sequence stratigraphy of the Oligo-Miocene Asmari Formation in SW Iran. Facies, 52, 41-51.

Warraich, M.Y., Ogasawara, K., Nishi, H., 2000. Late Paleocene to early Eocene planktic foraminiferal biostratigraphy of the Dungan Formation, Sulaiman Range, central Pakistan. Paleontological Research, 4, 275-301.

Wilson, M.E., J., Vecsei, A., 2005. The apparent paradox of abundant foramol facies in low latitudes: their environmental significance and effect on platform development. Earth-Science Reviews, 69, 133-168.

Wright, V.P., 1986. Facies sequences on a carbonate ramp: the Carboniferous Limestone of South Wales. Sedimentology, 33, 221-241.

Yordanova, E.K., Hohenegger, J., 2002. Taphonomy of larger foraminifera: relationships between living individuals and empty tests on flat reef slopes (Sesoko Island, Japan). Facies, 46, 169-203.

Zachos, J., Pagani, M., Sloan, L., Thomas, E., Billups, K., 2001. Trends, rhythms, and aberrations in global climate 65 Ma to present. science, 292, 686-693.

Zamagni, J., Mutti, M., Košir, A., 2008. Evolution of shallow benthic communities during the Late Paleocene–earliest Eocene transition in the Northern Tethys (SW Slovenia). Facies, 54, 25-43.

Zivkovic, S., Babić, L., 2003. Paleoceanographic implications of smaller benthic and planktonic foraminifera from the Eocene Pazin Basin (Coastal Dinarides, Croatia). Facies, 49, 49-60.